

# Land use direction based on landslide susceptibility levels in the Rongkong Watershed, South Sulawesi, Indonesia

TIRZA TIRSYAYU, ANDANG SURYANA SOMA, SAMUEL ARUNG PAEMBONAN

Faculty of Forestry, Universitas Hasanuddin. Jl. Perintis Kemerdekaan Km. 10, Tamalanrea, Makassar 90245, South Sulawesi, Indonesia

Manuscript received: 7 October 2024. Revision accepted: 11 February 2025.

**Abstract.** *Tirsyayu T, Soma AS, Paembonan SA. 2025. Land use direction based on landslide susceptibility levels in the Rongkong Watershed, South Sulawesi, Indonesia. Asian J For 9: 53-66.* Landslides, a common natural disaster in Indonesia, cause significant material and non-material losses. Mitigation efforts, including the provision of accurate information about landslide-prone areas and appropriate land-use recommendations, are crucial for minimizing their impact. This study, which analyzed landslide susceptibility using the frequency ratio method integrated with GIS technology, provides confidence in its methodology. The research, which began with data collection on landslide occurrences through imagery, identified 388 landslide points. These data were divided into two groups: validation data (20%) and training data (80%). The validation process, using the ROC curve, yielded an AUC value of 0.81, indicating the effectiveness of the frequency ratio method in predicting landslide occurrences in the Rongkong Watershed, South Sulawesi, Indonesia. The study revealed that parameters such as rainfall, slope gradient, land cover, elevation, lithology, curvature, and slope aspect significantly influence landslides in the Rongkong Watershed. In contrast, parameters such as distance from rivers, distance from roads, and NDVI had less influence. The study's findings, which classified landslide susceptibility levels as very high (1.32%), high (29.05%), and moderate (25.70%) based on the total area of the Rongkong Watershed, are of significant importance. They suggest that land use in areas with very high and high susceptibility should be designated for conservation or protected zones. In comparison, areas with moderate susceptibility can be utilized for limited and controlled cultivation, such as implementing agroforestry systems.

**Keywords:** Frequency ratio, landslide susceptibility, land use guidance, Rongkong Watershed

**Abbreviations:** AUC: Area Under the Curve, DEM: Digital Elevation Model, FR: Frequency Ratio, GIS: Geographic Information System, LSI: Landslide Susceptibility Index, NDVI: Normalized Difference Vegetation Index, ROC: Receiver Operating Characteristics, SPSS: Statistical Product and Service Solutions

## INTRODUCTION

The incidence of landslides in Indonesia has shown a worrying increase due to climate change, urbanization, and environmental degradation. According to the National Disaster Management Agency (BNPB 2022), there were 17,296 natural disasters in Indonesia over the last five years (2017-2021), with landslides ranking as the third most frequent disaster, totaling 3,811 cases. The highest number of landslide incidents occurred in 2020, with 1,152 cases resulting in 128 fatalities and causing other significant damages. Proactive mitigation efforts are crucial to reduce these impacts. Providing information about landslide-prone areas is one of the strategies to minimize landslide consequences. Landslide susceptibility levels can be calculated using the Frequency Ratio (FR) method (Cantarino et al. 2023; He et al. 2023; Khan et al. 2024), which evaluates the relationship between landslide-causing factors and landslide occurrences. The larger the ratio, the stronger the relationship between the landslide events and contributing factors (Soma and Kubota 2017). The factors analyzed using the frequency ratio method depend on the availability of field data, such as slope gradient, slope aspect, elevation, curvature, lithology, land cover, distance from rivers, distance from roads, rainfall intensity, and vegetation density.

The Rongkong Watershed, spanning approximately 107.10 km in length and covering an area of 172,878.68 hectares, is one of the regions frequently experiencing landslides. According to Al-Ghifary et al. (2016), the Rongkong Watershed is categorized as highly critical and prone to landslides due to its mountainous topography and high rainfall. Their study employed a scoring method focusing on the upstream area of the watershed. Kurniawan (2019) suggested increasing accuracy and adding parameters to improve landslide susceptibility assessments. Research by Gholami et al. (2019) found that the FR method has higher predictive accuracy than other methods. This method is also widely used for landslide susceptibility mapping (Jaafari et al. 2014; Meten et al. 2015; Efiang et al. 2021; KC et al. 2022; Keshri et al. 2023) and can be easily integrated with GIS technology. Geographic Information System is a computer-based system used to process spatial data or data that has geographic references. This technology is widely used in spatial analysis because it improves time efficiency and accuracy. Therefore, the application of the FR method is crucial to reducing researcher subjectivity, improving accuracy, incorporating additional parameters, and covering broader areas. This approach aims to assess entire watershed ecosystems, supporting safe and sustainable management while mitigating disaster risks exacerbated by increasing rainfall

intensity due to climate change. Furthermore, using watersheds as the unit of analysis, the causal relationships between upstream and downstream impacts can be clearly demonstrated (Narendra et al. 2021).

In addition to providing information on landslide-prone areas, offering proper land-use guidance is also an important effort to reduce the risk of landslide disasters. According to Arjomandi et al. (2021), one of the main contributors to environmental degradation is improper land-use allocation. Comprehensive watershed management within a unified ecosystem is essential for maintaining ecological balance, controlling floods and erosion, ensuring water quality, and supporting the sustainability of natural resources. A key approach to sustainable watershed management and development is the proper allocation of land use within the watershed. Land-use planning guidelines serve as a framework or policy designed to regulate and optimize land utilization in a given area to align with its function, capacity, and environmental conditions. In the context of disaster vulnerability, such as landslides, land-use planning plays a crucial role in minimizing risks by identifying safe areas for development and areas that should be preserved or left in their natural state. Improper land use, such as construction on steep slopes or deforestation, can significantly increase the risk of landslides and other natural disasters. Therefore, by incorporating landslide susceptibility into land-use planning, a balance can be achieved between development needs, environmental protection, and disaster risk reduction.

## MATERIALS AND METHODS

### Study area

This research was conducted from March to August 2024 in the Rongkong Watershed ( $2^{\circ} 21' 35'' - 2^{\circ} 56' 15''$  S

and  $119^{\circ} 51' 45'' - 120^{\circ} 23' 15''$  E), which encompasses the regions of North Luwu and Luwu Districts in South Sulawesi Province, Indonesia. Data processing was carried out at the Watershed Management Laboratory, Faculty of Forestry, Hasanuddin University, Makassar, Indonesia (Figure 1).

### Procedures

#### *Tools and materials*

The tools used include a laptop equipped with ArcGIS 10.8 and SPSS (Statistical Product and Service Solutions) applications, writing instruments, a camera, and a smartphone with mapping applications (SW Maps and Avenza Maps). The materials used include the Rongkong Watershed boundary map, administrative maps of Luwu and North Luwu Districts, Google Earth Pro imagery for landslide inventory from 2013-2023, Sentinel-2 imagery, the 2023 National DEM, rainfall data from 2013-2023, and the geological map of South Sulawesi.

#### *Landslide Inventory*

The landslide data for the Rongkong Watershed was obtained through the interpretation of Google Earth Pro imagery from 2013 to 2023. A total of 388 landslide points were identified, and a ground check was conducted to ensure the accuracy of the interpretation at several landslide points using a non-probability sampling technique. This technique does not provide equal opportunities for all population members to be selected. The type of sampling used was purposive sampling, where samples are chosen based on specific criteria such as accessibility to the location. This technique is among the most commonly used sampling methods (Palinkas et al. 2015). A total of 30 landslide points and 15 non-landslide points were used as research samples. The results of the ground check are shown in Figure 2.

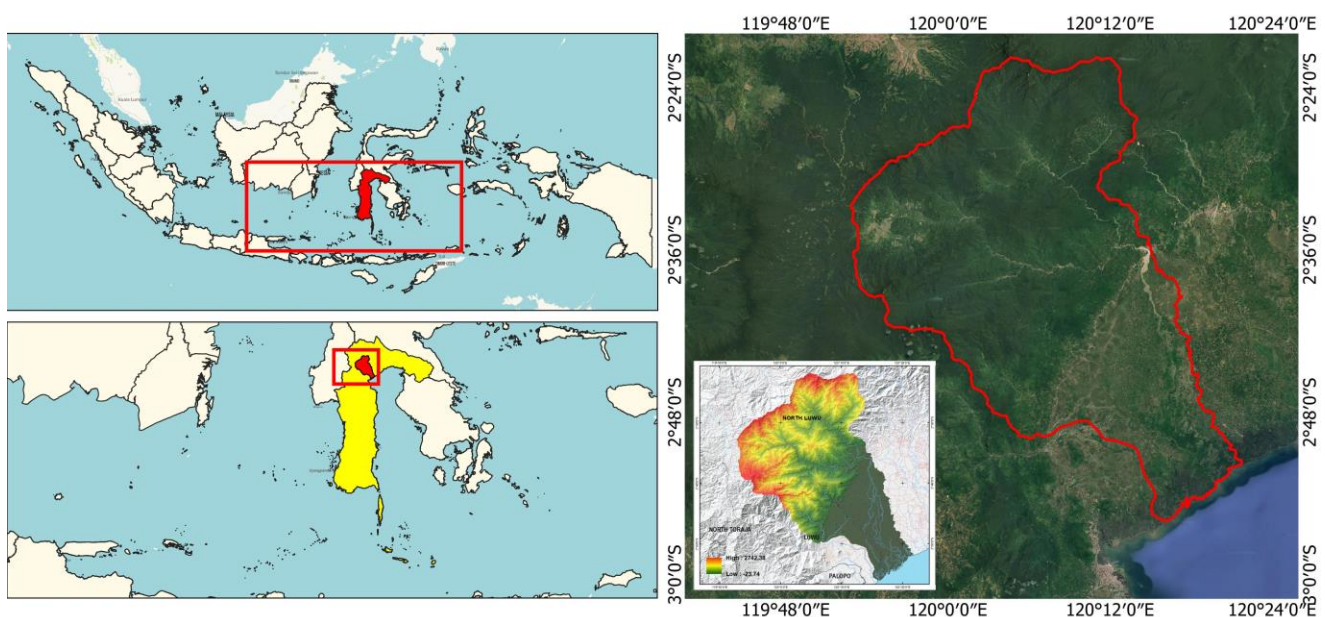


**Figure 1.** Map of the research area in the Rongkong Watershed, South Sulawesi Province, Indonesia



**Figure 2.** Landslides in the Rongkong Watershed. A. Interpretation results from Google Earth Pro; B-E. Ground check results

The validation of landslide occurrence data using the confusion matrix method and accuracy testing with overall accuracy showed that 91.11% of the data is accurate and acceptable, as it exceeds the 85% threshold set by Lillesand and Kiefer (2015). Landslide occurrence data were assigned a value of 1, and non-landslide data were assigned a value of 0, then converted into raster data with a pixel size of  $10 \times 10$  m. The total number of landslide pixels is 24,712 out of the total area of the Rongkong Watershed, which contains 17,287,886 pixels. This data was divided into two parts: 20% (4,943 pixels) for validation and 80% (19,769 pixels) for training.

#### *Data on the factors contributing to landslides*

This study analyzes the factors contributing to landslides, including rainfall, slope gradient, land cover, elevation, lithology, distance from rivers and roads, surface curvature, slope aspect, and vegetation density. Rainfall data from 2013 to 2023 was downloaded from NASA's website after identifying representative rainfall station points and stored in CSV format. The average annual rainfall was processed in ArcGIS using the Isohyet method and classified according to the Meteorology, Climatology, and Geophysics Agency (BMKG 2021) into four rainfall categories: low rainfall (0-1,500 mm), medium rainfall (1,500-3,000 mm), high rainfall (3,000-4,500 mm), and very high rainfall ( $>4,500$  mm).

Land cover data was generated through the interpretation of Sentinel-2A imagery. The interpretation was performed by analyzing patterns, tones, colors, and textures in the imagery and classifying them based on the 2010 National Standardization Agency guidelines. Field observations were conducted by selecting sample locations using the purposive sampling method, ensuring accessibility of the locations. Data validation was carried

out using the confusion matrix method, and accuracy testing with Overall Accuracy indicated a data accuracy of 92.5%. There are 12 types of land cover in the Rongkong Watershed: shrubs, primary dryland forest, secondary dryland forest, secondary mangrove forest, grassland, plantations, settlements, dryland agriculture, mixed dryland agriculture and shrubs, rice fields, rivers, and fishponds.

Elevation, slope gradient, distance from rivers, curvature, and slope aspect data were obtained from processing National DEM (Digital Elevation Model) data. Elevation data was classified based on the Minister of Public Works Regulation No. 20 of 2007 into the following classes:  $<500$  meters above sea level (masl), 500-1,500 masl, 1,500-2,500 masl, and  $>2,500$  masl. Slope gradient data was classified according to the Perdirjen BPDASPS No. P.4/V-SET/2013: flat ( $<8\%$ ), gentle (8-15%), moderately steep (16-25%), steep (26-40%), and very steep ( $>40\%$ ). Distance from rivers was categorized into four classes: 0-100 m, 100-200 m, 200-300 m, and  $>300$  m. Lithology data was derived from the geological map of South Sulawesi. Distance from roads was obtained by processing road data from the Geospatial Information Agency and classified into five classes:  $<500$  m, 500-1,000 m, 1,000-1,500 m, 1,500-2,000 m, and  $>2,000$  m.

Vegetation density was derived from Sentinel-2 imagery and assessed using the Normalized Difference Vegetation Index (NDVI) with the following formula (Jacquemart and Tiampo 2021; Niraj et al. 2023):

$$NDVI = \frac{NIR - RED}{NIR + RED}$$

Where: NIR refers to the band with a near-infrared wavelength (band 8), while RED refers to the band with a red wavelength (band 4). NDVI values are classified into five categories: non-vegetated (-1 to 0.25), sparse

vegetation (0.25 to 0.35), moderately dense vegetation (0.35 to 0.45), dense vegetation (0.45 to 0.50), and very dense vegetation (0.50 to 1). NDVI values range from -1 to 1 (Yengoh et al. 2015; Marsujitullah et al. 2023; Martinez and Labib 2023; Rashid et al. 2023). A value of -1 indicates a non-vegetated classification, whereas a value of 1 represents a very dense vegetation classification.

#### Data limitations and bias control strategies

The historical landslide event database is often incomplete or poorly documented, and there are data gaps in certain years, making it difficult to analyze trends consistently and comprehensively. This study introduces an innovative combined approach and integrates existing historical data with remote sensing data, such as satellite imagery and more recent field information, to address this limitation. This novel approach significantly improves the accuracy of the landslide susceptibility analysis, reflecting a more comprehensive condition.

#### Landslide susceptibility level analysis

The landslide susceptibility level is calculated based on the influence of rainfall, slope gradient, land cover, elevation, rock type/lithology, distance from rivers, distance from roads, surface curvature, slope aspect, and vegetation density on landslide occurrences, analyzed using the frequency ratio method with the following formula (Soma and Kubota 2017):

$$FR = \frac{P_{xL}(nm) / \sum P_{nxL}}{Pixel(nm) / \sum P_{nx}}$$

Where: FR stands for Frequency Ratio;  $P_{xL}$  refers to the number of landslide pixels in class  $n$  of parameter  $m$  (nm);  $Pixel$  represents the number of pixels in class  $n$  of parameter  $m$  (nm);  $\sum P_{nxL}$  is the total pixels of parameter  $m$ ; and  $\sum P_{nx}$  is the total pixels of the area. The larger the ratio exceeds 1, the stronger the relationship between landslide occurrences and the causal factor. Conversely, if the ratio is less than 1, the relationship between landslide occurrences and that factor is weak (Pradhan and Lee 2010). The Landslide Susceptibility Index (LSI) is created

by mapping all factors into raster maps based on their FR values, which are then summed using the formula (Abbasa et al. 2024; Gulbet and Getahun 2024):

$$LSI = \sum FR$$

#### Data validation

Data validation is intended to evaluate a classification model. The validation process uses the ROC (Receiver Operating Characteristics) curve, calculated using SPSS software. The ROC curve displays the AUC (Area Under Curve) value. AUC evaluation results are classified according to Rasyid et al. (2016) as follows: fail (0.50-0.60), poor (0.60-0.70), fair (0.70-0.80), good (0.80-0.90), and excellent (0.90-1.00). The data used include landslide events divided into two sets: 20% for assessing the model's predictive capability and 80% for evaluating the model's success. The validation results (Figure 3) show identical AUC values for both the model prediction rate (20%) and the model success rate (80%), at 0.806 or 0.81.

According to Rasyid et al. (2016), an AUC value within the range of 0.80-0.90 indicates that a model performs well. In this case, the frequency ratio method is considered effective in predicting landslide occurrences in the Rongkong Watershed.

## RESULTS AND DISCUSSION

#### Results of the frequency ratio analysis of landslide contributing factors in the Rongkong Watershed

The factors causing landslides are extracted into landslide data points, and their ratio to landslide occurrences is calculated. The FR value indicates the extent of a factor's influence on landslide occurrences. An FR value of 1 represents the average FR value; if  $FR > 1$ , it means the factor is correlated with landslide occurrences. Conversely, if  $FR < 1$ , the factor has minimal influence. The higher the FR value, the greater its impact on landslide occurrences (Huang et al. 2021; Sahrane et al. 2023). The FR value for each factor can be found in Table 1.

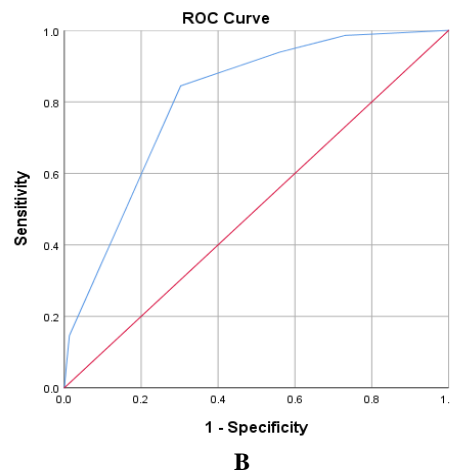
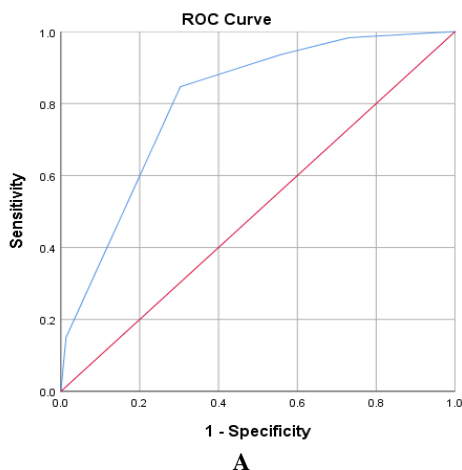


**Figure 3.** The ROC curve. A. Model Prediction Rate (20%) and B. Model Success Rate (80%)**Table 1.** The FR values of the factors contributing to landslides in the Rongkong Watershed, South Sulawesi, Indonesia

Parameter	Class	PxCL	% PxCL	PnXL	% PnXL	FR	
Rainfall (mm/year)	3,370.36	19,523	98.76	13,008,802	75.25	1.31	
	3,389.49	85	0.43	610,461	3.53	0.12	
	3,413.81	77	0.39	415,767	2.41	0.16	
	3,433.59	0	0.00	2,617,272	15.14	0.00	
	3,441.69	84	0.42	634,761	3.67	0.12	
	Total	19,769	100	17,287,063	100		
Slope (%)	0-8	235	1.19	4,339,796	25.10	0.05	
	8-15	347	1.76	933,749	5.40	0.32	
	16-25	873	4.42	1,448,739	8.38	0.53	
	26-40	4,395	22.23	4,556,209	26.36	0.84	
	>40	13,919	70.41	6,008,570	34.76	2.03	
	Total	19,769	100	17,287,063	100		
Land Cover	Shrubland	2,853	14.43	230,694	1.33	10.81	
	Primary Dryland Forest	1,671	8.45	814,697	4.71	1.79	
	Secondary Dryland Forest	13,761	69.61	9,267,173	53.61	1.30	
	Secondary Mangrove Forest	0	0.00	27,678	0.16	0.00	
	Grassland	51	0.26	1,557	0.01	28.64	
	Plantation	366	1.85	1,748,136	10.11	0.18	
	Settlement	0	0.00	398,278	2.30	0.00	
	Dryland Farming	5	0.03	1,615,109	9.34	0.00	
	Dryland Farming Mixed with Shrubs	680	3.44	933,678	5.40	0.64	
	Rice Field	261	1.32	1,478,531	8.55	0.15	
	River	121	0.61	301,517	1.74	0.35	
	Ponds	0	0.00	470,015	2.72	0.00	
	Total	19,769	100	17,287,063	100		
	Elevation (masl)	<500	1,159	5.86	7,207,798	41.69	0.14
		500-1500	15,352	77.66	7,207,675	41.69	1.86
1500-2500		3,252	16.45	2,852,047	16.50	1.00	
>2500		6	0.03	19,543	0.11	0.27	
Total		19,769	100	17,287,063	100		
Lithology	Latimojong Formation	174	0.88	797,799	4.62	0.19	
	Matano Formation	0	0.00	9,478	0.05	0.00	
	Ultramafic Complex	0	0.00	128,385	0.74	0.00	
	Alluvium	0	0.00	4,292,413	24.83	0.00	
	Barufu Tufa	78	0.39	543,098	3.14	0.13	
	Toraja Formation	214	1.08	512,469	2.96	0.37	
	Intrusive Rocks	0	0.00	1,296	0.01	0.00	
	Dondo Suit	16,834	85.15	7,626,040	44.11	1.93	
	Lamasi Volcano Rocks	2,469	12.49	3,376,085	19.53	0.64	
	Total	19,769	100	17,287,063	100		
	Distance from the river (m)	0-100	410	2.07	1,012,573	5.86	0.35
100-200		628	3.18	928,857	5.37	0.59	
200-300		850	4.30	883,972	5.11	0.84	
>300		17,881	90.45	14,461,661	83.66	1.08	
Total		19,769	100	17,287,063	100		
Distance from the road (m)	<500	1,443	7.30	4,525,896	26.18	0.28	
	500-1000	885	4.48	2,029,977	11.74	0.38	
	1000-1500	822	4.16	1,449,588	8.39	0.50	
	1500-2000	57	0.29	1,402,114	8.11	0.04	
	>2000	16,562	83.78	7,879,488	45.58	1.84	
Total	19,769	100	17,287,063	100			
Curvature	Concave	1187	6.00	676,138	3.91	1.54	
	Flat	10,361	52.41	8,251,754	47.73	1.10	
	Convex	8221	41.59	8,359,171	48.36	0.86	
Total	19,769	100	17,287,063	100			
Slope aspect	Flat	26	0.13	30,950	0.18	0.73	
	North	1,791	9.06	2,088,612	12.08	0.75	
	Northeast	2,746	13.89	2,135,194	12.35	1.12	
	East	3,224	16.31	2,396,859	13.87	1.18	
	Southeast	3,749	18.96	2,728,425	15.78	1.20	
	South	3,258	16.48	2,443,406	14.13	1.17	
	Southwest	2,306	11.66	1,998,299	11.56	1.01	
	West	1,272	6.43	1,724,967	9.98	0.64	
	Northwest	1,397	7.07	1,740,351	10.07	0.70	
	Total	19,769	100	17,287,063	100		
	Vegetation density	Non-Vegetated	744	3.76	701,002	4.06	0.93
Sparse Vegetation		450	2.28	313,993	1.82	1.25	
Moderately Dense Vegetation		467	2.36	380,781	2.20	1.07	
Dense Vegetation		294	1.49	188,867	1.09	1.36	

Very Dense Vegetation  
Total

17,814  
19,769

90.11  
100

15,702,420  
17,287,063

90.83  
100

0.99

Based on Table 1, it is evident that each factor has a different FR value, indicating that not all factors have the same level of correlation with landslide occurrences in the Rongkong watershed. The map of landslide-causing factors in the Rongkong Watershed can be seen in Figure 4. The FR value for each landslide-causing factor is presented in the graph below (Figure 5).

According to Hontus (2016), rainfall is a natural factor that plays an important role in landslide events. Rainfall is the dominant factor controlling slope stability (Zhang et al. 2019; Alsubal et al. 2019; Farooq and Akram 2021; Chellamuthu and Ganapathy 2024). High rainfall can increase the water pressure in the soil. Water that permeates the soil saturates it, reducing the soil's bearing capacity and increasing the risk of landslides (Gallage et al. 2021; Poddar and Roy 2024). High rainfall can also expand the soil's porosity. Water that seeps into the soil fills the pores, weakening the soil structure and making it more susceptible to mass movement. An increase in precipitation in a region will lead to more frequent landslide occurrences.

Based on the rainfall data processing from the last 10 years (2013-2022), the rainfall data for the Rongkong

Watershed ranges between 3,370.36 and 3,441.69 mm/year, which falls into the high rainfall category (3,000-4,500 mm/year). The corresponding FR value, which indicates the potential for landslide events, is shown in Figure 5.A. Figure 5.A also presents a surprising finding: while still categorized as high, a rainfall of 3,370.36 mm/year has an FR value of 1.31, the highest in the lowest class. This unexpected result underscores the strong relationship between landslide occurrences and rainfall. It suggests the influence of other factors, such as the predominantly very steep slope steepness and the land cover, including grasslands and shrubs.

Slope steepness has a significant influence on the potential for landslides (Guo et al. 2021; Tesfa and Woldearegay 2021). Steeper slopes exert greater pressure on the soil material, increasing the likelihood of mass movement downwards. According to the study by Roback et al. (2018), the highest landslides occur at the junction of steep slopes. The steeper the slope, the more likely a landslide will occur (Diara et al. 2022; Ma et al. 2022; Arumugam et al. 2023; Xie et al. 2023). The FR value of slope steepness in the Rongkong Watershed can be seen in Figure 5.B.

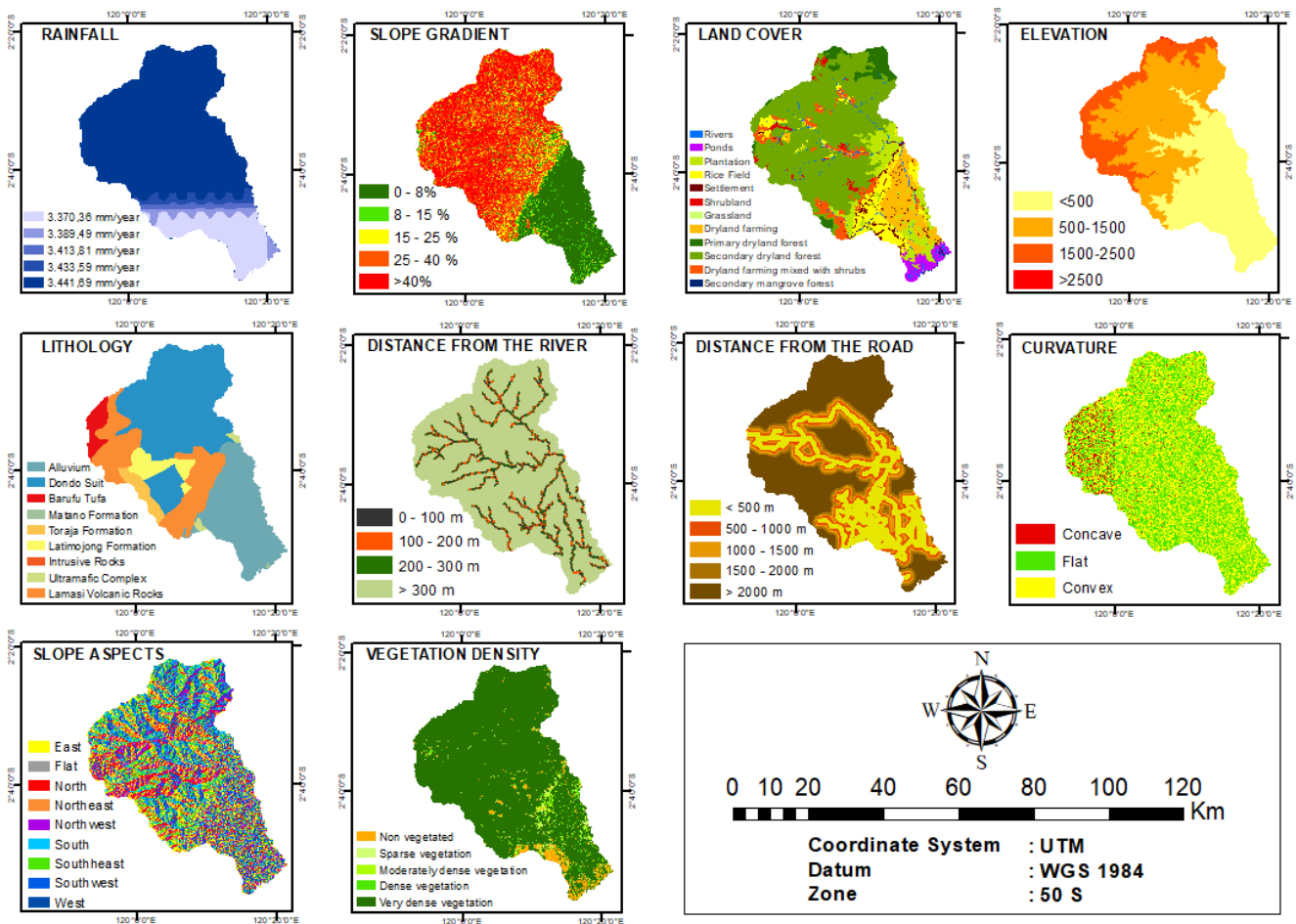


Figure 4. Map of landslide triggering factors in the Rongkong Watershed, South Sulawesi, Indonesia

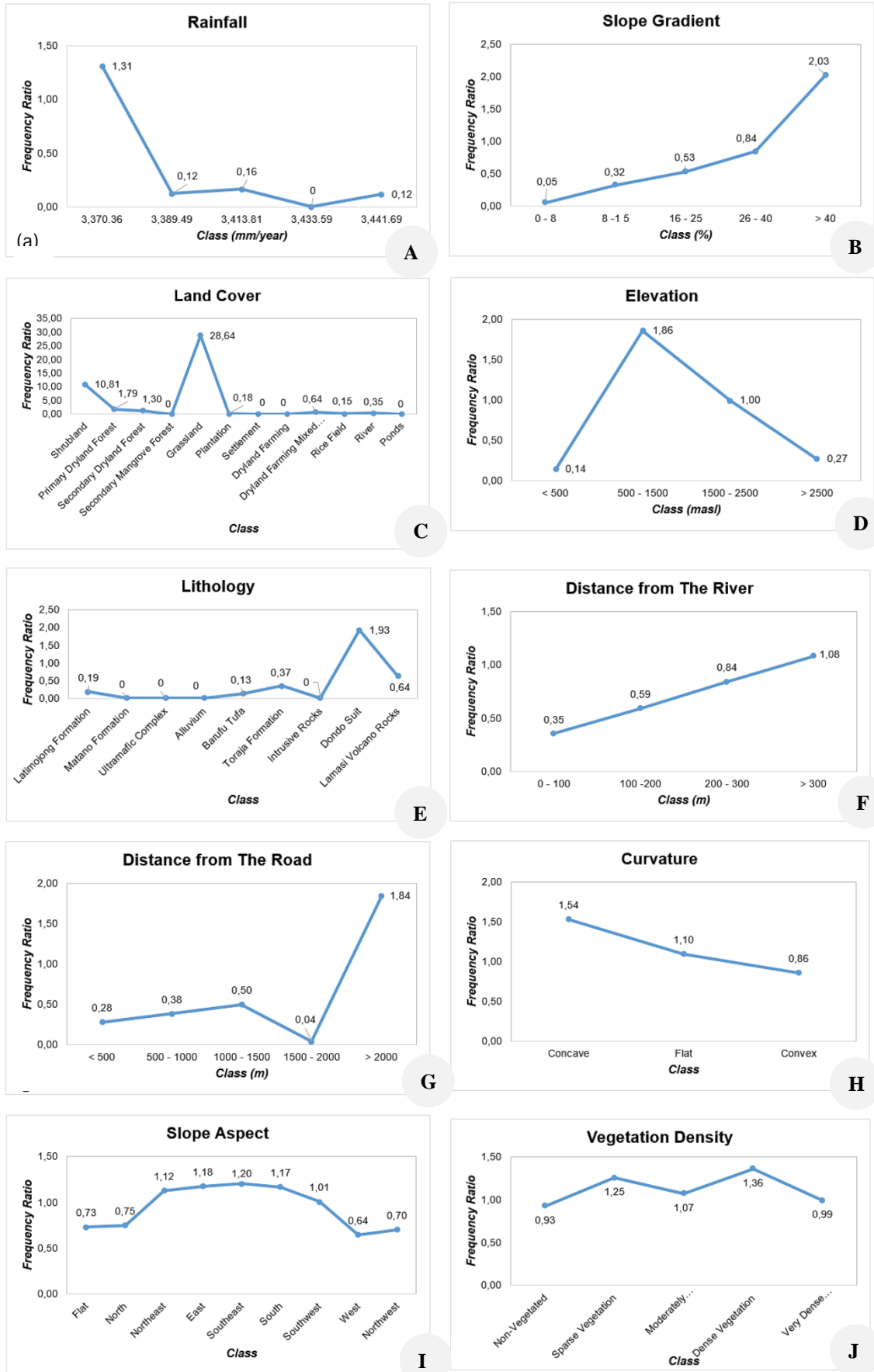


Figure 5. Graph of FR values for landslide-causing factors

At slopes >40% (very steep), the FR value is >1, specifically 2.03, indicating a strong relationship with landslide occurrences. Meanwhile, the slope classes of steep, moderately steep, gentle, and flat have FR values <1, indicating a low correlation. This aligns with the study by Tang et al. (2015), which found that landslide concentration increases with steeper slope angles. Slopes steeper than 20° are highly prone to landslides (Acosta-Quesada and Quesada-Román 2024). Additionally, other factors, such as high rainfall and land cover (grasslands and shrubs), have a significant impact on landslide occurrences on very steep slopes.

Land covered with dense vegetation and strong roots tends to have a lower risk of landslides because it can absorb rainwater and prevent material saturation on slopes, especially on steep slopes (Jeong et al. 2017). Forests with strong root systems can stabilize the soil and help maintain slope stability (Soma and Kubota 2017; Sujatha et al. 2023). The roots of vegetation can help maintain soil stability by reinforcing the soil structure and preventing erosion (Dorairaj and Osman 2021; Jafari et al. 2022; Gong et al. 2024; Lann et al. 2024).

Based on Figure 5.C, land cover types with an FR value >1 include grasslands, shrubs, primary dryland forests, and secondary dryland forests. Grasslands, covering an area of 15.57 ha, have an FR value of 28.64; shrubs, with an area of 2,306.94 ha, have an FR value of 10.81; followed by primary dryland forests, covering 814,697 ha with an FR value of 1.79, and secondary dryland forests, covering 9,267,173 ha, with an FR value of 1.30.

Landslides can occur in areas with land cover types such as bare land, fields, shrubs, and grasslands. According to Hurlimann et al. (2022), root strength is higher in forests than in grasslands and shrubs. In a previous study by Abedin (2020), most landslide events occurred in areas with shrub and grassland cover. Shrubs and grasslands have a less robust root system to anchor the soil, resulting in lower soil stability and making landslides more likely. Although secondary dryland forests are often covered by tree vegetation, landslides can still occur due to disturbances or changes from their original condition caused by human activities. Unlike primary dryland forests, landslides can still happen in these areas, even without human activities, due to other factors influencing soil stability. It's crucial to understand that steep slopes and heavy rainfall are critical factors that can trigger landslides, underscoring the urgency of studying these elements. Most of the primary dryland forests in the Rongkong Watershed are located on very steep slopes with high rainfall.

The higher the elevation of an area, the greater the potential gravitational energy, which makes soil and rocks more active (Wu et al. 2023). In higher areas, groundwater pressure is higher due to more rainfall infiltrating the soil. High groundwater pressure can cause the soil to become more saturated and soft, which increases the likelihood of landslides. High elevations, especially on steep slopes, tend to support the occurrence of landslides (Li et al. 2021; Dunham et al. 2022).

Figure 5.D presents a graph of the FR values for the elevation of the Rongkong Watershed. The elevation class

with an FR value greater than 1 is between 500 and 1,500 meters above sea level (1.86). Meanwhile, the elevation from 1,500 to 2,500 masl shows a value of 1, which represents the average FR value; unlike the landslide study by Li et al. (2021), landslide occurrences in the Rongkong Watershed decrease at elevations of 1500 meters and above, marked by a decline in the FR value. A similar finding was reported in the study by Zhou et al. (2016), which stated that landslides are more frequent at mid-elevations, specifically between 900-1,300 masl and 1,200-2,000 masl. Landslides at these mid-elevations occur due to human activities, such as deforestation, which reduces or even eliminates vegetation that helps maintain slope stability. This is further exacerbated by the high rainfall and steep slopes in the Rongkong Watershed, which facilitate the occurrence of landslides.

According to the Ministry of Public Works Regulation Number 22/PRT/M/2007, one of the factors that contribute to landslides is the type of rock/lithology. Lithology is an important controlling factor (Bahrami et al. 2019; Pourghasemi et al. 2020; Wu et al. 2020; Conforti and Ietto 2021; Yu et al. 2021; Rahaman et al. 2024). The strength of the rock can determine how easily or how difficult it is for the rock to break or shift. Rocks with fragile or fragmented structures are more prone to landslides because they are more easily affected by pressure and ground movement. On steeper slopes, more material is crushed for certain types of material, leading to larger landslides (Katz et al. 2014). In the Rongkong Watershed, there are nine types of rock formations: Latimojong Formation, Matano Formation, Ultramafic Complex, Alluvium, Tufa Barufu, Toraja Formation, Intrusive Rocks, Suit Dondo, and Lamasi Volcano Rocks. The FR values for each lithology class are shown in Figure 5.E.

Based on Figure 5.E, the Suit Dondo rock type has an FR value greater than 1, specifically 1.93, indicating a strong correlation with landslide occurrences in the Rongkong Watershed. Suit Dondo rocks generally have a coarse to medium texture and high hardness. Landslides can occur when hard rocks undergo weathering (Saputra and Heriyadi 2019; Silwal et al. 2024). According to Komadja et al. (2020), weathering of rocks causes slope instability, which triggers landslides. Especially on very steep slopes and with high rainfall, these rocks may fracture and lead to landslides.

Based on Figure 5.F, it can be seen that the distance from the river with an FR value greater than 1 is greater than 300 meters (1.08). According to Cheng et al. (2021), the distance from the river is one of the factors that significantly influences landslides. Slopes near rivers are more prone to landslides (Hidayah et al. 2017; Hua et al. 2020; Ali et al. 2021; Mahalingam and Kim 2021; Naik and Palakuzhiyil 2024). softening the soil, which weakens slope stability. A different finding was observed in the Rongkong Watershed, where landslides were more frequent at distances greater than 300 meters. Similarly, in the study by Abedin (2020), the distance from the river had little influence on landslide occurrences. Although the distance from the river is far, landslides in the Rongkong Watershed can still occur due to other factors, such as very

steep slopes, high rainfall, and land cover in the form of shrubs and grasslands.

The distance from roads within the Rongkong Watershed is shown in Figure 5.G, the road >2,000 meters (1.84). This value indicates a high correlation between landslide occurrences and the distance from the road in the >2000 m class. According to Hidayah et al. (2017), the distance between the road and the slope can trigger landslides due to vehicle traffic around the slope. The closer the slope is to the road, the greater the likelihood of a landslide (Teimouri and Nalivan 2020; Ye et al. 2022). In contrast to the Rongkong Watershed, landslides in this area are more frequent in that the distance from the road did not significantly affect landslide occurrences, as indicated by the lowest weight value among all the factors. This is also consistent with the research of Abedin (2020), which found that most landslides occur within 2000 meters of the road. This is likely due to other factors influencing landslide occurrences in the area, such as high rainfall and slope steepness, which is dominated by moderate to very steep gradients.

There are three forms of the Earth's surface: convex, indicated by positive values; concave, indicated by negative values; and flat, indicated by zero values. Concave areas of the Earth's surface tend to have a higher risk of landslides compared to convex areas. This is because concave slopes can retain more water after heavy rainfall and hold it for longer periods, causing the soil to reach saturation and lose strength, making it more prone to landslides. Zhuang et al. (2018) stated that landslides are more common on concave slopes. In Figure 5.H, curvature (concave) classes with an FR value greater than 1 are the concave and flat classes. The concave class has an FR value of 1.54, while the flat class has an FR value of 1.10, indicating a strong correlation with landslide occurrences in the Rongkong Watershed. This is due to the possibility of flat areas forming in highlands as a result of geological processes such as sedimentation or erosion. Flat areas on steep slopes, such as terraces, tend to collect rainwater, causing the soil to become saturated and triggering landslides, especially during periods of high rainfall.

One significant factor affecting landslide occurrences is the slope aspect (Gorokhovich and Vustianiuk 2021; Qi et al. 2021); varying levels of rainfall, sunlight, and wind influence slopes facing different directions. Slopes that receive more rainfall tend to be more vulnerable to landslides compared to those facing other directions (Cellek 2021). Additionally, wind direction can also affect landslides. Indirectly, strong winds can exert pressure on slopes from a specific direction, increasing the stress on the soil or rock material on that slope, thereby disrupting slope stability and increasing the risk of landslides, especially if the slope is already unstable.

Figure 5.I is a graph showing the FR values for slope aspect. The FR value greater than 1 is found in the southeast slope direction (1.20), followed by the east direction (1.18), south direction (1.17), northeast direction (1.12), and southwest direction (1.01). It can be observed that the FR value increases from the north to the southeast

and then decreases again toward the northwest direction. This is consistent with the study by Naseer et al. (2021), which found that slopes facing the sun are generally more exposed to direct sunlight, accelerating weathering processes and increasing the risk of landslides. South-facing slopes are also the most susceptible to landslides (Bahadur et al. 2020; Li et al. 2021). When the sun is in the south, rainfall tends to be higher due to the large amount of evaporation from the Indian Ocean. Zhuang et al. (2018) also found that landslides were more dominant on slopes facing southeast. Wu et al. (2020) added that east-facing slopes are more prone to landslides.

Vegetation can help maintain slope stability by preventing erosion and soil movement. The denser the vegetation, the stronger the soil is bound by plant roots, thereby reducing the likelihood of landslides. The FR value of vegetation density is presented in Figure 5.J.

According to the study by Deng et al. (2022), most landslides occur on slopes with sparse vegetation and are less frequent in areas with high vegetation density. High vegetation cover plays a crucial role in reducing landslide risk because it helps support slope stability and aids in landslide mitigation. Gholami et al. (2019) also stated that vegetation density significantly influences landslide occurrence, with landslide frequency decreasing as vegetation density increases. However, this study found that the highest FR values were actually in areas with dense vegetation, with a value of 1.36, followed by areas with sparse vegetation (1.25) and moderately dense vegetation (1.07). This is certainly influenced by other factors at the study site, such as steep slopes, which dominate the area with a very steep gradient covering 60,089.67 hectares, and high rainfall. It's important to note that the vegetation density index or NDVI, while useful in providing information about the presence or density of vegetation, cannot provide information about the quality of the vegetation, particularly the species diversity in the study area, which could help prevent landslides. This highlights the need for further research and development in this area.

## Discussion

### *Landslide susceptibility in the Rongkong Watershed*

The landslide susceptibility map of the Rongkong Watershed (Figure 6) was created based on the LSI values, which represent the levels of very low, low, moderate, high, and very high landslide susceptibility (Chen et al. 2014). Figure 7 shows the percentage of landslide susceptibility in the Rongkong Watershed. It is calculated by dividing the area of the susceptibility class by the total area of the Rongkong watershed, multiplied by 100.

The very low susceptibility class covers an area of 46,588.50 ha (26.95%) and includes 79 villages. The largest area of low susceptibility is in Lawewe Village (Baebunta Selatan District), with 2,824.812 ha, followed by Wara Village (Malangke Barat District), with 2,687.800 ha, and Lembang-lembang Village (Baebunta Selatan District) with 2,266.173 ha. Dryland agriculture, rice fields, and settlements dominate this class.

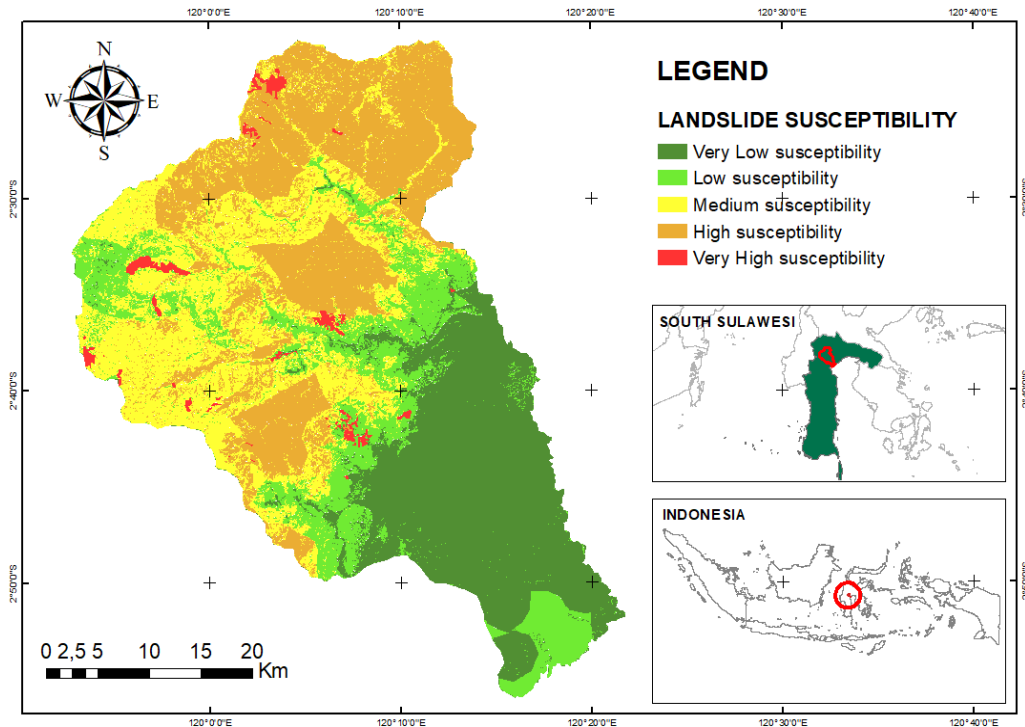


Figure 6. Landslide susceptibility map of the Rongkong Watershed, South Sulawesi, Indonesia

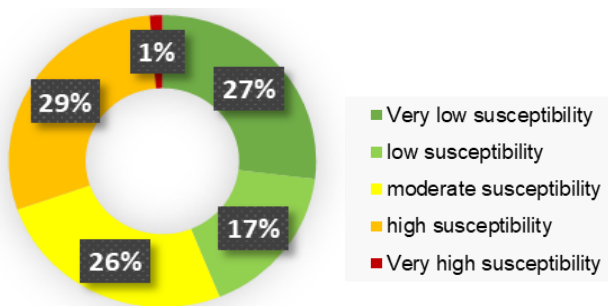


Figure 7. Landslides susceptibility level percentage in Rongkong Watershed, South Sulawesi, Indonesia

The low susceptibility class covers an area of 29,339.90 ha (16.97%) and includes 75 villages. The village with the largest area of low susceptibility is Malimbu Village (Sabbang District) at 2,983.20 ha, followed by Pombakka Village (Malangke Barat District) at 2,247.23 ha, and Tandung Village (Sabbang District) at 2,061.51 ha. Secondary dryland forest cover, plantations, and mixed dryland agriculture and shrubland dominate this class.

The moderate susceptibility level covers an area of 44,436.06 ha (25.70%) and includes 28 villages. The village with the highest moderate landslide susceptibility is Tandung Village (Sabbang District) at 7,425.09 ha, followed by Malimbu Village (Sabbang District) at 3,416.22 ha and Siteba Village (Walenrang Utara District) at 3,363.79 ha. This class is dominated by secondary dryland forest cover, mixed dryland agriculture and shrubland, and primary dryland forest.

The high susceptibility class covers an area of 50,226.70 ha (29.05%) and includes 23 villages. Maipi Village (Masamba District) ranks first for the highest area of high landslide susceptibility, measuring 9,278.84 ha, followed by Kanandede Village (Limbung District) at 7,975.83 ha and Baebunta Village (Baebunta District) at 6,519.30 ha. This class is also dominated by secondary dryland forest cover, primary dryland forest, and mixed dryland agriculture and shrubland.

The very high susceptibility class encompasses an area of 2,287.52 ha (1.32%) and includes 15 villages. The village with the largest area is Maipi Village (Masamba District) at 587.48 ha, followed by Pongko Village (Walenrang Utara District) at 322.48 ha, and Tandung Village (Sabbang District) at 286.84 ha. This class is dominated by shrubland cover, secondary dryland forest, and grassland. Although the very high susceptibility class represents only 1.34% of the total area of the Rongkong Watershed, the area of 2,287.52 ha is not insignificant. Furthermore, the high susceptibility class has the largest area, reaching 29.05%, and the moderate susceptibility class covers 25.70%. Therefore, it is essential to remain vigilant regarding the potential for landslides to occur.

*Land use direction for the Rongkong Watershed*

Land use is one of the factors that influences environmental conditions. Improper land use can have detrimental effects on the environment, including increased erosion, heightened surface runoff, and an elevated risk of landslides and flooding. Determining land use directions based on landslide susceptibility levels is a crucial step in spatial planning and disaster risk management. According

to Eker and Aydin (2016), a risk-based approach is essential in land use planning to minimize the impacts of landslides. Furthermore, Lillesand and Kiefer (2015) stated that disaster risk management is a key component of sustainable development strategies aimed at reducing losses and supporting community resilience. Landslide susceptibility maps can be utilized as a supportive tool in decision-making to implement better land use planning (Roccati et al. 2021).

The direction of land use is based on the results of the analysis of landslide susceptibility levels in the Rongkong Watershed. It takes into account the types of land use in areas categorized by their susceptibility to landslides. Land use that does not conform to spatial planning guidelines in landslide-prone areas will be directed to prevent landslide risks. Based on the levels of landslide susceptibility in the Rongkong Watershed, land use directions are provided in accordance with spatial planning guidelines outlined in Ministerial Regulation No. 22/PRT/M/2007. In areas with very high and high landslide susceptibility, there are settlements, rice fields, grasslands, plantations, and shrublands. These areas are designated as protected areas or conservation zones. Agricultural activities and the development of residential centers, along with supporting facilities for social and economic activities, should be avoided, except for facilities that directly improve environmental quality, such as drainage systems and other environmental infrastructure networks.

In areas with moderate landslide susceptibility containing rice fields, settlements, plantations, shrublands, and grasslands, land use is directed to function as limited controlled cultivation areas, such as the implementation of agroforestry systems. Activities related to the components of spatial structure should adhere to the environmental carrying capacity and comply with the provisions set forth in Government Regulation No. 27 of 1999 concerning Environmental Impact Assessment.

In areas with low and very low landslide susceptibility, land can be utilized for residential activities, mining, production forests, urban forests, plantations, agriculture, fisheries, livestock, tourism, or other activities while still adhering to Government Regulation No. 27 of 1999 concerning Environmental Impact Assessment. In the Rongkong Watershed, land use in areas with low and very low susceptibility levels is already in accordance with regulations.

The findings regarding the landslide susceptibility level provide important information to the local community about potential risks in their area, particularly for the communities in Maipi, Kanandede, and Baebunta Villages, which are identified as areas with very high landslide risk. With a better understanding, the community can become more alert and prepared for potential disasters, such as avoiding certain activities in high-risk areas. Additionally, by providing accurate and applicable information to the local community, this research helps them make wiser, sustainability-oriented decisions, thereby minimizing the negative impacts of future landslides. The suggested land use guidance is crucial for minimizing natural disaster risks, improving land productivity, and supporting the

community's well-being. With the implementation of the recommended strategies, land management can be conducted more effectively and efficiently, providing long-term benefits in terms of economy, environment, and society and offering hope for a safer future.

However, socio-economic challenges may arise in implementing these recommendations. Most of the people in landslide-prone areas depend on land use for agriculture, livestock, or settlement. Relocation or land-use changes could lead to the risk of losing livelihoods and increase economic burdens. Additionally, limited access to resources, such as funding for implementing mitigation practices or supporting technologies, could present significant barriers. Therefore, an approach involving the local community, such as providing economic incentives, ongoing education, and government support, is essential to overcoming these challenges and ensuring the successful implementation of the recommendations.

In conclusion, land use directions are established to control landslides, with areas of very high and high susceptibility directed to become protected or conservation areas. In contrast, areas with moderate susceptibility are designated for limited cultivation with strict controls, such as the implementation of agroforestry systems. The results of this study can serve as a primary basis in spatial planning, particularly in identifying and designating protected or conservation areas in regions with very high and high landslide susceptibility. Local governments need to strengthen regulations and supervision of development in these areas to minimize disaster risks. Additionally, this study emphasizes the importance of synergistic collaboration between the government, non-governmental organizations, academia, and local communities in designing and implementing comprehensive risk mitigation strategies. This approach ensures that the research findings are not merely academic documents but are translated into policies and concrete actions that effectively reduce disaster impacts.

## ACKNOWLEDGEMENTS

We would like to express our gratitude to all parties who have contributed to this research. We wish to extend our thanks to the Faculty of Forestry at Hasanuddin University, Indonesia for providing the necessary facilities and resources. We are grateful to our colleagues and friends for their moral support and constructive criticism.

## REFERENCES

- Abbasa H, Khana AA, Hussaina D, Khanb G, Hassan SN, Kulsooma I, Bazai SU. 2024. Landslide inventory and landslide susceptibility mapping for China Pakistan Economic Corridor (CPEC)'s main route (Karakorum Highway). *J Appl Emerg Sci* 11 (1): 18-30. DOI: 10.36785/jaes.111461.
- Abedin J, Rabby YW, Hasanx I, Akter H. 2020. An investigation of the characteristics, causes, and consequences of 13 June, 2017, landslides in Rangamati District Bangladesh. *Geoenviron Dis* 7: 23. DOI: 10.1186/s40677-020-00161-z.

- Acosta-Quesada M, Quesada-Román A. 2024. Landslides and flood hazard mapping using geomorphological methods in Santa Ana, Costa Rica. *Intl J Dis Risk Reduct* 113: 104882. DOI: 10.1016/j.ijdr.2024.104882.
- Al-Ghifary A, Malamassam D, Bachtiar B. 2016. Pemetaan tingkat kerawanan longsor di Sub DAS Rongkong Hulu, DAS Rongkong, Kabupaten Luwu Utara. [Skripsi]. Hasanuddin University, Makassar. [Indonesian]
- Ali M, Chu HJ, Chen YC, Ullah S. 2021. Machine learning in earthquake- and typhoon-triggered landslide susceptibility mapping and critical factor identification. *Environ Earth Sci* 80: 233. DOI: 10.1007/s12665-021-09510-z.
- Alsabal S, Sapari NB, Harahap ISH, Al-Bared MA. 2019. A review on mechanism of rainwater in triggering landslide. *IOP Conf Ser: Mat Sci Eng* 513 (1): 012009. DOI: 10.1088/1757-899X/513/1/012009.
- Arumugam T, Kinattinkara S, Velusamy S, Shanmugamoorthy M, Murugan S. 2023. GIS based landslide susceptibility mapping and assessment using weighted overlay method in Wayanad: A part of Western Ghats, Kerala. *Urban Clim* 49: 101508. DOI: 10.1016/j.uclim.2023.101508.
- Arjomandi A, Mortazavi SA, Khalilian S, Garizi AZ. 2021. Optimal land-use allocation using MCDM and SWAT for the Hablehroud Watershed, Iran. *Land Use Policy* 100: 104930. DOI: 10.1016/j.landusepol.2020.104930.
- Bahadur PB, Rai P, Katel P, Khadka A. 2020. Landslide Hazard Mapping in Panchase Mountain of Central Nepal. *Environ Nat Resour* 18 (4): 387-399. DOI: 10.32526/enrj.18.4.2020.37.
- Bahrami S, Rahimzadeh B, Khaleghi S. 2019. Analyzing the effects of tectonic and lithology on the occurrence of landslide along Zagros ophiolitic suture: a case study of Sarv-Abad, Kurdistan, Iran. *Bull Eng Geol Environ* 79: 1619-1637. DOI: 10.1007/s10064-019-01639-3.
- BMKG. 2021. Peta Rata-rata Curah Hujan dan Hari Hujan periode 1991-2020 Indonesia. Pusat Informasi Perubahan Iklim BMKG, Jakarta. [Indonesian]
- BNPB. 2022. Data Informasi Bencana Indonesia. Badan Nasional Penanggulangan Bencana. Diakses dari Pusat Data Informasi dan Komunikasi Kebencanaan (Pusdatinkom): <https://dibi.bnpb.go.id/>. [Indonesian]
- Cantarino I, Carrion M, Martínez-Ibáñez V, Gielen E. 2023. Improving landslide susceptibility assessment through frequency ratio and classification methods—Case study of Valencia Region (Spain). *Appl Sci* 13 (8): 5146. DOI: 10.3390/app13085146.
- Cellek S. 2021. The effect of aspect on landslide and its relationship with other parameters. In: Zhang Y, Cheng Q (eds.). *Landslides*. InTech Open, London. DOI: 10.5772/intechopen.99389.
- Chellamuthu SN, Ganapathy GP. 2024. Quantifying the impact of changing rainfall patterns on landslide frequency and intensity in the Nilgiris District of Western Ghats, India. *Prog Dis Sci* 23: 100351. DOI: 10.1016/j.pdisas.2024.100351.
- Chen W, Li W, Hou E, Zhao Z, Deng N, Bai H, Wang D. 2014. Landslide susceptibility mapping based on GIS and information value model for the Chencang District of Baoji, China. *Arab J Geosci* 7: 4499-4511. DOI: 10.1007/s12517-014-1369-z.
- Cheng YS, Yu TT, Son NT. 2021. Random forests for landslide prediction in Tsengwen River Watershed, Central Taiwan. *Remote Sens* 13 (2): 199. DOI: 10.3390/rs13020199.
- Conforti M, Ietto F. 2021. Modeling shallow landslide susceptibility and assessment of the relative importance of predisposing factors, through a GIS-based statistical analysis. *Geosciences* 11 (8): 333. DOI: 10.3390/geosciences11080333.
- KC D, Dangi H, Hu L. 2022. Assessing landslide susceptibility in the northern stretch of Arun Tectonic Window, Nepal. *Civil Eng* 3 (2): 525-540. DOI: 10.3390/civileng3020031.
- Deng J, Ma C, Zhang Y. 2022. Shallow landslide characteristics and its response to vegetation by example of July 2013, extreme rainstorm, Central Loess Plateau, China. *Bull Eng Geol Environ* 81: 100. DOI: 10.1007/s10064-022-02606-1.
- Diara IW, Saifulloh M, Suyarto R. 2022. Spatial distribution of landslide susceptibility in new road construction Mengwitani-Singaraja, Bali-Indonesia: Based on geospatial data. *Intl J Geomate* 23 (90): 95-103. DOI: 10.21660/2022.96.3320.
- Dorairaj D, Osman N. 2021. Present practices and emerging opportunities in bioengineering for slope stabilization in Malaysia: An overview. *PeerJ* 9 (10): e10477. DOI: 10.7717/peerj.10477.
- Dunham AM, Kiser E, Kargel JS, Haritashya UK, Watson CS, Shugar DH, DeCelles PG. 2022. Topographic control on ground motions and landslides from the 2015 Gorkha Earthquake. *Geophys Res Lett* 49 (10): e2022GL098582. DOI: 10.1029/2022GL098582.
- Efiong J, Eni DI, Obiefuna J, Etu S. 2021. Geospatial modelling of landslide susceptibility in Cross River State of Nigeria. *Sci Afr* 14: 01032. DOI: 10.1016/j.sciaf.2021.e01032.
- Eker R, Aydin A. 2016. Landslides susceptibility assessment of forest roads. *Eur J For Eng* 2 (2): 54-60.
- Fadilah N, Arsyad U, Soma AS. 2019. Analisis tingkat kerawanan longsor menggunakan metode frekuensi rasio di Daerah Aliran Sungai Bialo. *Jurnal Perennial* 15 (1): 42-50. DOI: 10.24259/perennial.v15i1.6317. [Indonesian]
- Farooq S, Akram MS. 2021. Landslide susceptibility mapping using information value method in Jhelum Valley of the Himalayas. *Arabian J Geosci* 14 (10): 824. DOI: 10.1007/s12517-021-07147-7.
- Gallage C, Abeykoon T, Uchimura T. 2021. Instrumented model slopes to investigate the effects of slope inclination on rainfall-induced landslides. *Soils Found* 61 (1): 160-174. DOI: 10.1016/j.sandf.2020.11.006.
- Gholami M, Ghachkanlu E, Khosravi K, Pirasteh S. 2019. Landslide prediction capability by comparison of frequency ratio, fuzzy gamma and landslide index method. *J Earth Syst Sci* 128: 42. DOI: 10.1007/s12040-018-1047-8.
- Gong C, Ni D, Liu Y, Li Y, Huang Q, Tian Y, Zhang H. 2024. Herbaceous vegetation in slope stabilization: A comparative review of mechanisms, advantages, and practical applications. *Sustainability* 16 (17): 7620. DOI: 10.3390/su16177620.
- Gorokhovich Y, Vustianiuk A. 2021. Implications of slope aspect for landslide risk assessment: A case study of Hurricane Maria in Puerto Rico in 2017. *Geomorphology* 391: 107874. DOI: 10.1016/j.geomorph.2021.107874.
- Gulbet E, Getahun B. 2024. Landslide susceptibility mapping using frequency ratio and analytical hierarchy process method in Awabel Woreda, Ethiopia. *Quat Sci Adv* 16: 100246. DOI: 10.1016/j.qsa.2024.100246.
- Guo X, Fu B, Du J, Shi P, Li J, Li Z, Fu H. 2021. Monitoring and assessment for the susceptibility of landslide changes after the 2017 Ms 7.0 Jiuzhaigou earthquake using the remote sensing technology. *Front Earth Sci* 9: 633117. DOI: 10.3389/feart.2021.633117.
- He W, Chen G, Zhao J, Lin Y, Qin B, Yao W, Cao Q. 2023. Landslide susceptibility evaluation of machine learning based on information volume and frequency ratio: A case study of Weixin County, China. *Sensors* 23 (5): 2549. DOI: 10.3390/s23052549.
- Hidayat A, Paharuddin, Massinai MA. 2017. Analisis rawan bencana longsor menggunakan metode AHP (Analytical Hierarchy Process) di Kabupaten Toraja Utara. *Jurnal Geoelebes* 1 (1): 1-4. DOI: 10.20956/geoelebes.v1i1.1772. [Indonesian]
- Hontus AC. 2016. Excess moisture - A major reason why producing landslides. *Sci Pap Ser Manag Econ Eng Agric Rural Dev* 16 (4): 171-180.
- Hua Y, Wang X, Li Y, Xu P, Xia W. 2020. Dynamic development of landslide susceptibility based on slope unit and deep neural networks. *Landslides* 18: 281-302. DOI: 10.1007/s10346-020-01444-0.
- Huang F, Ye Z, Jiang SH, Huang J, Chang Z, Chen J. 2021. Uncertainty study of landslide susceptibility prediction considering the different attribute interval numbers of environmental factors and different data-based models. *CATENA* 202: 105250. DOI: 10.1016/j.catena.2021.105250.
- Hurlimann M, Guo Z, Puig-Polo C, Medina V. 2022. Impacts of future climate and land cover changes on landslide susceptibility: regional scale modelling in the Val d'Aran region (Pyrenees, Spain). *Landslides* 19: 99-118. DOI: 10.1007/s10346-021-01775-6.
- Jacquemart M, Tiampo K. 2021. Leveraging time series analysis of radar coherence and normalized difference vegetation index ratios to characterize pre-failure activity of the Mud Creek landslide, California. *Nat Hazards Earth Syst Sci* 21: 629-642. DOI: 10.5194/nhess-21-629-2021.
- Jaafari M, Tahmoures M, Ehteram M, Ghorbani M, Panahi F. 2022. Slope stabilization methods using biological and biomechanical measures. In: Jafari M, Tahmoures M, Ehteram M, Ghorbani M, Panahi F (eds.). *Soil Erosion Control in Drylands*. Springer, Cham. DOI: 10.1007/978-3-031-04859-3\_6.
- Jeong S, Lee K, Kim J, Kim Y. 2017. Analysis of Rainfall-Induced Landslide on Unsaturated Soil Slopes. *Sustainability* 9 (7): 1280. DOI: 10.3390/su9071280.

- Katz O, Morgan JK, Aharonov E, Dugan B. 2014. Controls on the size and geometry of landslides: Insights from discrete element numerical simulations. *Geomorphology* 220: 104-113. DOI: 10.1016/j.geomorph.2014.05.021.
- Keshri D, Sarkar K, Chatto SL. 2023. Landslide susceptibility mapping in parts of Aglar watershed, Lesser Himalaya based on frequency ratio method in GIS environment. *J Earth Syst Sci* 133: 1. DOI: 10.1007/s12040-023-02204-z.
- Khan I, Kainthola A, Bahuguna H, Asgher M. 2024. Comparative landslide susceptibility assessment using information value and frequency ratio bivariate statistical methods: a case study from Northwestern Himalayas, Jammu and Kashmir, India. *Arab J Geosci* 17: 231. DOI: 10.1007/s12517-024-12022-2.
- Komadja GC, Pradhan SP, Roul AR, Adebayo B, Baptiste JH, Glodji LA, Onwuulu AP. 2020. Assessment of stability of a Himalayan road cut slope with varying degrees of weathering: A finite-element-model-based approach. *Heliyon* 6 (11): e05297. DOI: 10.1016/j.heliyon.2020.e05297.
- Kurniawan R. 2019. Determination of landslide susceptibility level using scoring method in Pugung Area, Tanggamus. *IOP Conf Ser: Mater Sci Eng* 620 (1): 012126. DOI: 10.1088/1757-899X/620/1/012126.
- Lann T, Bao H, Lan H, Zheng H, Yan C, Peng J. 2024. Hydro-mechanical effects of vegetation on slope stability: A review. *Sci Total Environ* 926: 171691. DOI: 10.1016/j.scitotenv.2024.171691.
- Li M, Ma C, Du C, Yang W, Lyu L. 2021. Landslide response to vegetation by example of July 25-26, 2013, extreme rainstorm, Tianshui, Gansu Province, China. *Bull Eng Geol Environ* 80: 751-764. DOI: 10.1007/s10064-020-02000-9.
- Lillesand TM, Kiefer RW, Chipman JW. 2015. *Remote Sensing and Image Interpretation* (7th ed.). Wiley, New York.
- Ma S, Shao X, Xu C. 2022. Characterizing the distribution pattern and a physically based susceptibility assessment of shallow landslides triggered by the 2019 heavy rainfall event in Longchuan County, Guangdong Province, China. *Remote Sens* 14 (17): 4257. DOI: 10.3390/rs14174257.
- Mahalingam R, Kim B. 2021. Factors affecting occurrence of landslides induced by the M7.8 April 2015, Nepal Earthquake. *KSCE J Civil Eng* 25: 78-91. DOI: 10.1007/s12205-020-0508-1.
- Marsujitullah, Kaligis DA, Manggau FX. 2023. Health analysis of rice plants based on the Normalized Difference Vegetation Index (NDVI) value in image of unmanned aircraft (case study of Merauke - Papua Selatan). *Eng Technol J* 8 (2): 1986-1991. DOI: 10.47191/etj/v8i2.04, I.F. - 7.136.
- Martinez ADI, Labib S. 2023. Demystifying normalized difference vegetation index (NDVI) for greenness exposure assessments and policy interventions in urban greening. *Environ Res* 220: 115155. DOI: 10.1016/j.envres.2022.115155.
- Meten M, Bhandary NP, Yatabe R. 2015. Effect of landslide factor combinations on the prediction accuracy of landslide susceptibility maps in the Blue Nile Gorge of Central Ethiopia. *Geoenviro Dis* 2: 9. DOI: 10.1186/s40677-015-0016-7.
- Naik D, Palakuzhiyil Y. 2024. Landslide Susceptibility Mapping using Geospatial framework -A Study of Pinder Basin, Chamoli District, Uttarakhand, India. DOI: 10.21203/rs.3.rs-4006670/v1.
- Narendra BH, Siregar CA, Dharmawan IW, Sukmana A, Pratiwi, Pramono IB, Basuki TM, Nugroho HY, Supangat AB, Purwanto, Setiawan O. 2021. A review on sustainability of watershed management in Indonesia. *Sustainability* 13 (19): 11125. DOI: 10.3390/su131911125.
- Naseer S, Haq TU, Khan A, Tanoli JI, Khan NG, Qaiser FR, Shah ST. 2021. GIS-based spatial landslide distribution analysis of district Neelum, AJ&K, Pakistan. *Nat Hazards* 106: 965-989. DOI: 10.1007/s11069-021-04502-5.
- Niraj K, Singh A, Shukla D. 2023. Effect of the normalized difference vegetation index (NDVI) on GIS-enabled bivariate and multivariate statistical models for landslide susceptibility mapping. *J Indian Soc Remote Sens* 51: 1739-1756. DOI: 10.1007/s12524-023-01738-5.
- Palinkas LA, Horwitz SM, Green CA, Wisdom JP, Duan N, Hoagwo K. 2015. Purposeful sampling for qualitative data collection and analysis in mixed method implementation research. *Adm Policy Ment Health* 42 (5): 533-544. DOI: 10.1007/s10488-013-0528-y.
- Peraturan Menteri PU No 22/PRT/M/2007 Tentang Pedoman Penataan Ruang. Pemerintah Indonesia, Jakarta. [Indonesian]
- Poddar I, Roy R. 2024. Application of GIS-based data-driven bivariate statistical models for landslide prediction: A case study of highly affected landslide prone areas of Teesta River basin. *Quat Sci Adv* 13: 100150. DOI: 10.1016/j.qsa.2023.100150.
- Pourghasemi HR, Kornejady A, Kerle N, Shabani F. 2020. Investigating the effects of different landslide positioning techniques, landslide partitioning approaches, and presence-absence balances on landslide susceptibility mapping. *CATENA* 187: 104364. DOI: 10.1016/j.catena.2019.104364.
- Pradhan B, Lee S. 2010. Landslide susceptibility assessment and factor effect analysis: Back propagation artificial neural networks and their comparison with Frequency Ratio and Bivariate Logistic Regression Modeling. *Environ Mod Software* 25: 747-759. DOI: 10.1016/j.envsoft.2009.10.016.
- Qi T, Zhao Y, Meng X, Chen G, Dijkstra T. 2021. AI-based susceptibility analysis of shallow landslides induced by heavy rainfall in Tianshui, China. *Remote Sens* 13 (9): 1819. DOI: 10.3390/rs13091819.
- Rahaman A, Dondapati A, Gupta S, Raj R. 2024. Leveraging artificial neural networks for robust landslide susceptibility mapping: A geospatial modeling approach in the ecologically sensitive Nilgiri District, Tamil Nadu. *Geohazard Mech* 2 (4): 258-269. DOI: 10.1016/j.ghm.2024.07.001.
- Rashid M, Sheik M, Haque A, Siddique M, Habib M, Patwary MA. 2023. Salinity-induced change in green vegetation and land use patterns using remote sensing, NDVI, and GIS techniques: A case study on the southwestern coast of Bangladesh. *Case Stud Chem Environ Eng* 7: 100314. DOI: 10.1016/j.cscee.2023.100314.
- Rasyid A, Bhandary N, Yatabe R. 2016. Performance of frequency ratio and logistic regression model in creating GIS based landslides susceptibility map at Lompobattang Mountain, Indonesia. *Geoenviro Dis* 3: 19. DOI: 10.1186/s40677-016-0053-x.
- Roback K, Clark MK, West AJ, Zekkos D, Li G, Gallen SF, Godt JW. 2018. The size, distribution, and mobility of landslides caused by the 2015 Mw7.8 Gorkha earthquake, Nepal. *Geomorphology* 301: 121-138. DOI: 10.1016/j.geomorph.2017.01.030.
- Roccati A, Paliaga G, Luino F, Faccini F, Turconi L. 2021. GIS-Based landslide susceptibility mapping for land use planning and risk assessment. *Land* 10 (2): 162. DOI: 10.3390/land10020162.
- Rosi A, Tofani V, Tanteri L, Stefanelli CT, Agostini A, Catani F, Casagli N. 2018. The new landslide inventory of Tuscany (Italy) updated with PS-InSAR: geomorphological features and landslide distribution. *Landslides* 15: 5-19. DOI: 10.1007/s10346-017-0861-4.
- Sahrane R, Bounab A, Kharim Y. 2023. Investigating the effects of landslides inventory completeness on susceptibility mapping and frequency-area distributions: Case of Taounate province, Northern Morocco. *CATENA* 220 (B): 106737. DOI: 10.1016/j.catena.2022.106737.
- Saputra RA, Heriyadi B. 2019. Analisis klasifikasi massa batuan dan potensi longsor pada area pit timur tambang terbuka PT. Allied Indo Coal Jaya, Kota Sawalunto, Sumatera Barat. *Jurnal Bina Tambang* 4 (3): 207-217. DOI: 10.24036/bt.v4i3.105700. [Indonesian]
- Silwal B, Gyawali B, Yoshida K. 2024. Geochemical and mineralogical analysis of low-grade metamorphic rocks and their response to shallow landslide occurrence in Central Nepal. *Geoenviro Dis* 11: 37. DOI: 10.1186/s40677-024-00301-9.
- Soma AS, Kubota T. 2017. The performance of land use change causative factor on landslide susceptibility map in Upper Ujung-Loe Watersheds South Sulawesi, Indonesia. *J Geomat Plan* 4 (2): 157-170. DOI: 10.14710/geoplanning.4.2.157-170.
- Sujatha E, Sudarsan J, Nithiyantham S. 2023. A review on sustainable reinforcing techniques to stabilize slopes against landslides. *Intl J Environ Sci Technol* 20: 13873-13882. DOI: 10.1007/s13762-023-04832-w.
- Tang C, Ma G, Chang M, Li W, Zhang D, Jia T, Zhou Z. 2015. Landslides triggered by the 20 April 2013 Lushan earthquake, Sichuan Province, China. *Eng Geol* 187: 45-55. DOI: 10.1016/j.enggeo.2014.12.004.
- Teimouri M, Nalivan O. 2020. Susceptibility zoning and prioritization of the factors affecting landslide using MaxEnt, Geographic Information System and remote sensing models (Case study: Lorestan Province). *Hydrogeomorphology* 6 (21): 155-179.
- Tesfa C, Woldearegay K. 2021. Characteristics and susceptibility zonation of landslides in Wabe Shebelle Gorge, south eastern Ethiopia. *J Afr Earth Sci* 182: 104275. DOI: 10.1016/j.jafrearsci.2021.104275.
- Wu W, Xu C, Wang X, Tian Y, Deng F. 2020. Landslides triggered by the 3 August 2014 Ludian (China) Mw 6.2 earthquake: An updated inventory and analysis of their spatial distribution. *J Earth Sci* 31: 853-866. DOI: 10.1007/s12583-020-1297-7.

- Wu X, Song Y, Chen W, Kang G, Qu R, Wang Z, Chen H. 2023. Analysis of geological hazard susceptibility of landslides in Muli County based on random forest algorithm. *Sustainability* 15 (5): 4328. DOI: 10.3390/su15054328.
- Xie C, Huang Y, Li L, Li T, Xu C. 2023. Detailed Inventory and Spatial Distribution Analysis of Rainfall-Induced Landslides in Jiexi County, Guangdong Province, China in August 2018. *Sustainability* 15 (18): 13930. DOI: 10.3390/su151813930.
- Ye CM, Wei R, Ge Y, Li Y, Junior J, Li J. 2022. GIS-based spatial prediction of landslide using road factors and random forest for Sichuan-Tibet Highway. *J Mt Sci* 19: 461-476. DOI: 10.1007/s11629-021-6848-6.
- Yengoh GT, Dent D, Olsson L, Tengberg AE, Tucker III CJ. 2015. Use of the Normalized Difference Vegetation Index (NDVI) to Assess Land Degradation at Multiple Scales. Springer, Cham. DOI: 10.1007/978-3-319-24112-8.
- Yu X, Zhang K, Song Y, Jiang W, Zhou J. 2021. Study on landslide susceptibility mapping based on rock-soil characteristic factors. *Sci Rep* 11: 15476. DOI: 10.1038/s41598-021-94936-5.
- Zhang K, Wang S, Bao H, Zhao X. 2019. Characteristics and influencing factors of rainfall-induced landslide and debris flow hazards in Shaanxi Province, China. *Nat Hazards Earth Syst Sci* 19 (1): 93-105. DOI: 10.36785/jaes.111461.
- Zhou SH, Chen G, Fang L. 2016. Distribution pattern of landslides triggered by the 2014 Ludian earthquake of China: Implications for regional threshold topography and the seismogenic fault identification. *Geo-Information* 5 (4): 46. DOI: 10.3390/ijgi5040046.
- Zhuang J, Peng J, Wang G, Javed I, Wang Y, Li W. 2018. Distribution and characteristics of landslide in Loess Plateau: A case study in Shaanxi province. *Eng Geol* 236: 89-96. DOI: 10.1016/j.enggeo.2017.03.001.